UNIVERSCI

Materials Chemistry Horizons

Research article

Ultrasonic Assisted Extraction of Grape Seeds: Structural Characterization and Biological Implications

Walid El Hotaby, Bahaa Hemdan, Wafa I. Abdel-Fattah, Ghareib W. Ali*

Received: 08/09/2024 **Resubmitted:** 18/11/2024 **Accepted:** 27/11/2024 **Published:** 07/12/2024 **DOI:** 10.61186/MCH.2024.1068 OPEN ACCESS

ABSTRACT

Recently, grapes by-products have great attention due to their unique antioxidant activity and biological promoting effects. Grape seeds powder was greenly extracted by ultrasonic probe at a sonication power of 6 kJ within 10 minutes. Physico-chemical characterizations were performed for grape seed powder through FESEM, XRD, and XPS. Biological implications including bactericidal and anticancer activities were conducted for the extract. Moreover, the antioxidant activity of the obtained extract was examined. The bactericidal activity was investigated against both *Gram-positive* and *Gram-negative* bacteria. The obtained results confirmed the efficacy of the facile green applied route in extracting grapes seed without affecting its desired structural and biological activities. Therefore, the extract recorded an excellent free radical scavenging activity of 92% to compete with the ascorbic acid. Moreover, it proves promising bactericidal activity against tested bacterial strains with clear zones up to 25 mm. The grapes seed extract possesses an inhibition percentage of up to 78.2 against pancreatic cancer cells.

Keywords: Grape-seeds, Ultrasonic-extraction, Bactericidal activity, Anticancer evaluation

INTRODUCTION

Grapes are considered one of the world's most important fruit crops with unique antioxidant, anti-inflammatory, anti-cancer, and anti-aging activities because of their ubiquitous and abundant production of the secondary metabolite group [1, 2]. However, Grape seeds are treated as agricultural waste despite their rich polyphenol content. Instead, they can be reused and converted into valuable economic turns via numerous scientific processes [3, 4]. Grape polyphenols are mostly present in the seeds, with a high ratio between 60 to 70 percent of their total extractable compounds. The series of non-polar (lipids) and semi-polar (phenolics) molecules highly accumulated in grape seeds is responsible for their bioactivities. Worldwide, grape seed extract is considered a natural source of polymeric and pro-anthocyanidins oligomeric. Pro-anthocyanidins, extracted from grapes seed, are defined to be procyanidins consisting of flavan–3-ols, as (+)-catechin, (−)-epicatechin, and (−)-epicatechin–3-gallate that linked through C4–C6 or C4–C8 bonds [5, 6]. Comparatively, grape seeds contain higher levels of monomeric, oligomeric, and polymeric flavanol content than grape skin [6–8]. Therefore, grape seeds exhibited a higher antioxidant activity with

*Corresponding author: wafaaghareib@gmail.com

participation in numerous physiological regulatory mechanisms making it a reliable candidate for the potential medical applications [9–11].

Flavonoids are proven to have promising anticancer activity through the reduction of cellular oxidative damage helping, therefore, the maintenance of intracellular antioxidant defenses via their free radical scavenging ability. Recently, several medicinal plants and their components have been applied for infectious disease treatment as Coptis chinensis Franch and Rhodomyrtus tomentosa. The flavonoids isolated from grape seeds exhibit promising bactericidal activity against different bacterial strains [12–15].

Ultrasound-assisted extraction is considered one of the non-conventional techniques that have been applied for the extraction of fruits' bioactive compounds [16–19]. It aims to improve the performance of conventional extraction routes, especially for the short processing time and the increased yield extraction [20, 21]. Ultrasound cavitation forces are responsible for its higher efficiency that involves bubbles implosion formed within the extracted medium. Accordingly, a rapid adiabatic compression of the gases and vapors originates within the cavities or bubbles. Therefore, high temperature and pressure are produced leading to cell wall rupture and facile access to the cellular content followed by an elevation in the analytic solubility and solvent penetration into the extraction matrix [22–24].

In this scenario, ultrasonic mediated extraction of grapes seeds is optimized to be applied for dual antioxidant and bactericidal applications.

MATERIALS AND METHODS

Materials

Roumy Ahmer (red) grapes were obtained from the local markets in Egypt, Citric acid and absolute ethanol 99.8% (Fisher Scientific UK) were utilized. Folin Ciocalteu reagent (Sigma Aldrich), Sodium carbonate (99.5, Merck), Sodium Nitrate (99.99, Merck), Aluminum chloride (99.99, Sigma Aldrich) and Sodium hydroxide (99.5, Merck) were used.

Methods

Preparation of Grape Seeds Extract (GSE)

The collected grape seeds were washed several times with tape water followed by distal water then dried in an oven (Mehmert, German) at 50^0C overnight. Further, the grape seeds were ground using a special die agitates mortar (Janke & Kunkel GmbH Co., Germany). The obtained fine seeds powder was immersed in a 3% alcoholic /citric acid solution (50% deionized water + 50 % absolute ethanol). The solution suspension was treated by ultrasonic (probe with a frequency of 20 kHz) irradiation for 10 minutes at 6K Joule. The treated solution media was filtered using filter paper (Whatman 4) and the clear solution was kept in the fridge for further analysis.

Structural Characterization and Biological Implications

Structural Characterization

Surface topology of the grapes seeds powder was investigated by field emission scanning electron microscope (FESEM) at the National Research Centre (Quanta FEG 250-type microscope equipped with an energy dispersive X-ray attachment EDAX/Genesis device). Moreover, X-ray powder diffraction (XRD) analysis was achieved using Cu K□ radiation (l = 1.5418 Å) at 0.3 S scanning speed (Philips X'pert Pro X-ray powder diffractometer). The applied current and voltage were 40 mA and 40 kV respectively. Additionally, the X-ray photoelectron Spectroscopy (XPS) technique was applied on an AXIS ULTRA DLD spectrometer with AlK-α radiation (hν = 1486.71 eV). An energy resolution of 0.48 eV was adjusted at 150Watt (W) with a pass energy of 16 electron volts (eV).

Biological Implications

Determination of Total Polyphenol Content

Total polyphenol content is determined according to the Folin Ciocalteu method described by Pastrana-Bonilla *et al.* 0.2 ml of each diluted sample is added to dilute Folin Ciocalteu reagent (1 ml, 10-fold). Post incubation for two minutes, sodium carbonate (0.8 ml, 7.5%) is added. While the extraction solution is replaced by distilled water for

blank at similar conditions. All samples are incubated for 30 minutes at room temperature. The absorbance of each solution is measured at 765 nm. The same procedure is repeated for all gallic acid solutions with a concentration range between 0 and 0.25 mg/ml [25, 26].

Determination of Total Flavonoid Content

Total flavonoids are measured by mixing 1 mL of the tested sample with 0.3 ml of $NaNO_2$ (5 %, w/v). After 5 minutes, 0.5 mL of $AlCl_3$ (2 %, w/v) is added. A standard flavonoid solution (100 µm) is used. Then, the tested sample is mixed and neutralized by 0.5 ml of 1 mole of NaOH standard solution post 6 minutes. The mixture is incubated at room temperature for 10 minutes. The absorbance was measured at the range of 300–600 nm against the blank, where $AlCl_3$ solution was substituted by water. Quercetin of concentration range 0–125-µg/ml is chosen as the standard for the expression of the results at 510 nm [27].

DPPH Free Radical Scavenging Test

Various concentrations ranged between 0–250 µg/ml of the extract and/or ascorbic acid (as a positive control) is mixed separately with 1 mL of DPPH% solution in ethanol (0.1 mM). The mixtures are dark and kept for 30 minutes then, the absorbance is measured at 517 nm [28]. The DPPH inhibition percentage is calculated by applying the following equation

$$\text{Inhibition}\% = \left(1 - \frac{A_s}{A_c}\right) \times 100, \tag{1}$$

where A_s is the absorbance of the DPPH% sample solution, and A_c is the absorbance of the DPPH% blank solution.

Bactericidal Activity

Antibacterial Susceptibility Testing (AST)

Using the Kirby-Bauer agar diffusion technique (disc and well diffusion), the assembled natural extract's bactericidal efficiency and zone of inhibition (ZOI) dimensions were explored towards 6 particular categories of bacterial pathogens. Three Gram-negative (GN) species including, *E.coli O157:H7, Pseudomonas aeruginosa,* and *Klebsiella pneumonia,* and three Gram-positive (GP) species including *Staphylococcus aureus, Bacillus subtilis,* and *Listeria monocytogenes* were applied in this study. According to the previous investigation done by Hemdan *et al.,* the targeted bacterial strains were regrown and sub-cultured by spreading the stocked culture onto nutrient agar [29].
Upon that surface of Mueller Hinton Agar (MHA) dishes, the formerly mentioned examined types were meticulously distributed with uniform cell suspension. The disc-diffusion assay was conducted in particular circumstances. The sterilized designed discs were maintained under sterile conditions for dryness after already being immersed using 50 µl of the generated natural extract at a 20 µg/mL dosage. Utilizing sterile clamping forceps, the moistened discs were then positioned on the MHA summit surface. Using a sterilized Cork borer with an internal diameter of 8 mm, boreholes in a thick layer of MHA medium were punched for the well-diffusion experiment. The prepared extract was aseptically injected through each hole at a fixed volume of 50µl. Vancomycin and Ciprofloxacin were employed as positive controls, and sterilized water functioned as the negative regulation. All dishes were then flipped over and left in an incubator at 37 °C. Using a digital caliper, the zone of inhibition (ZOI) readings throughout the discs and wells were measured [30]. According to Lavorgna *et al.* [31], the nonlinear dose-response modeling was applied to estimate the IC_{50} values and IC record (concentration levels that can destroy 50% of viable cells) for the extract utilizing GraphPad Prism programming Software.

Determination of Minimum Inhibitory Concentrations

Using a quantitative technique, the MIC values and effective dosage of the prepared extract were determined. The concentrations used ranged between 5 to 25 mg/ml. Three tubes are filled with the prepared natural extract solution (media containing the doses of the prepared natural extract), the prepared natural extract solution, and the positive control (media containing antibiotic inoculum). One mL of each tube was transmitted to Petri dishes after exposure to different retention times (10, 15, 30 min), and the proper quantity of agar medium was poured. Following that, all

implanted plates were incubated overnight at 37°C. The MIC values were confirmed by comparing the two types of control tubes. The results were offered as the means of three independent replicates [32].

The Pseudo-First-Order Kinetic Modeling

The following formula was applied to calculate the kinetic modeling to figure out the ratio of the original microbial cell densities (N0) to the total number of viable cells containing the required density of the prepared natural extract tests performed over numerous retention times (Nt), in order to estimate the dangerous values (k1) of each species of bacteria being taken into account [33].

$$\log (q_e - q_t) = \log q_e - \frac{K_1 t}{2.303}, \tag{2}$$

where k_1 ($1min^{-1}$) is the rate of inactivation, q_e ($\mu g.mL^{-1}$), and q_t ($\mu g.mL^{-1}$) are the amounts adsorbed at equilibrium and at time t (min), respectively. A straight line of ln (q_e—q_t) versus t suggested that this kinetic model applied to the data [28].

The Physiological Changes of Bacterial Strains

By adding 100 ml of bacterial culture to two test tubes each comprising 50 ml of sterile trypticase soy broth, we were able to assess the amount of basic variability in the multiplication and makeup of the bacterial isolates. One amongst them received an injection of the manufactured natural extract at its effective concentration (25 mg/mL), whereas the other served as the comparison group. Samples were taken every two hours for a full 24 hours (n = 12 readings) throughout all tubes that were deposited in a shaking incubator at 37 °C with a 200 rpm shaking [34].

Bacterial Growth Rate

A volume of sample (1 mL) was retrieved from each assigned tube to quantify each investigated bacterial strain's absorption spectrum at 600 nm using the spectrophotometer [35].

Estimation of amounts of released protein

The Bradford protein assay was applied to measure the quantities of liberated protein from damaged cells [36, 37].

ATP Bioluminescence Assay

ATP reflects a significant variability in the cell's activities while levels have dropped suddenly followed by cell killing. Bacterial energies and superior advantage have been determined by assessing the external ATP production that uses the luciferin-luciferase technique. The luminescence shapes and luminescence brightness were computed and recognized as relative fluorescence units using the ATP luminometer (RLU) [37, 38].

Anticancer Activity

In-vitro cytotoxicity studies were investigated against normal skin fibroblast normal cells (BJ1), Pancreatic cancer cell line (PACA2), Lung carcinoma cell line (A549) and breast cancer (MCF7) cell lines by MTT assay 3-[4, 5-dimethylthiazol–2- yl]–3, 5-diphenyltetrazolium bromide dye. In detail, the tested cells are inserted in a well plate at a specific density of 1 $\times 10^4$ cells per well. The media are inoculated with an antibiotic–anti–mycotic mixture (1%); composed of potassium penicillin (10,000 U mL^{-1}), streptomycin sulfate (10,000 µg/mL), amphotericin B (25µg/mL), and L-glutamine (1%, Bio west, USA). Further, the media are incubated at body temperature (37 °C) in a humidified atmosphere at 5% CO_2. Post-cell attachment, the media are replaced by the extracted sample for 72 hours. The cells are incubated within the MTT solution (5.0 mg/mL) at 37 °C for four hours. The developed purple formazan crystals are dissolved in 100µL dimethyl sulfoxide (DMSO) and recorded on an ELISA reader. The cell viability percentage is calculated following the below equation

$$\text{Viability}\% = \frac{\text{OD}_{\text{test}} - \text{OD}_{\text{blank}}}{\text{OD}_{\text{control}} - \text{OD}_{\text{blank}}} \times 100, \tag{3}$$

where

OD_{test}: The value of extract absorbance measured at 570 nm,
OD_{blank}: The value of blank absorbance measured at 570 nm,
$OD_{control}$: The negative control.

RESULTS AND DISCUSSIONS

Structural Characterization of Grape Seeds Extract Powder

Field Emission Scanning Electron Microscope (FESEM)

The surface morphology of the grape seeds extract powder was depicted using FESEM along with its EDAX (Figure 1). The figures show fiber bundles embedded within the grape seeds matrix. The diameter of the enlarged fibers ranged between 360–440 nm.

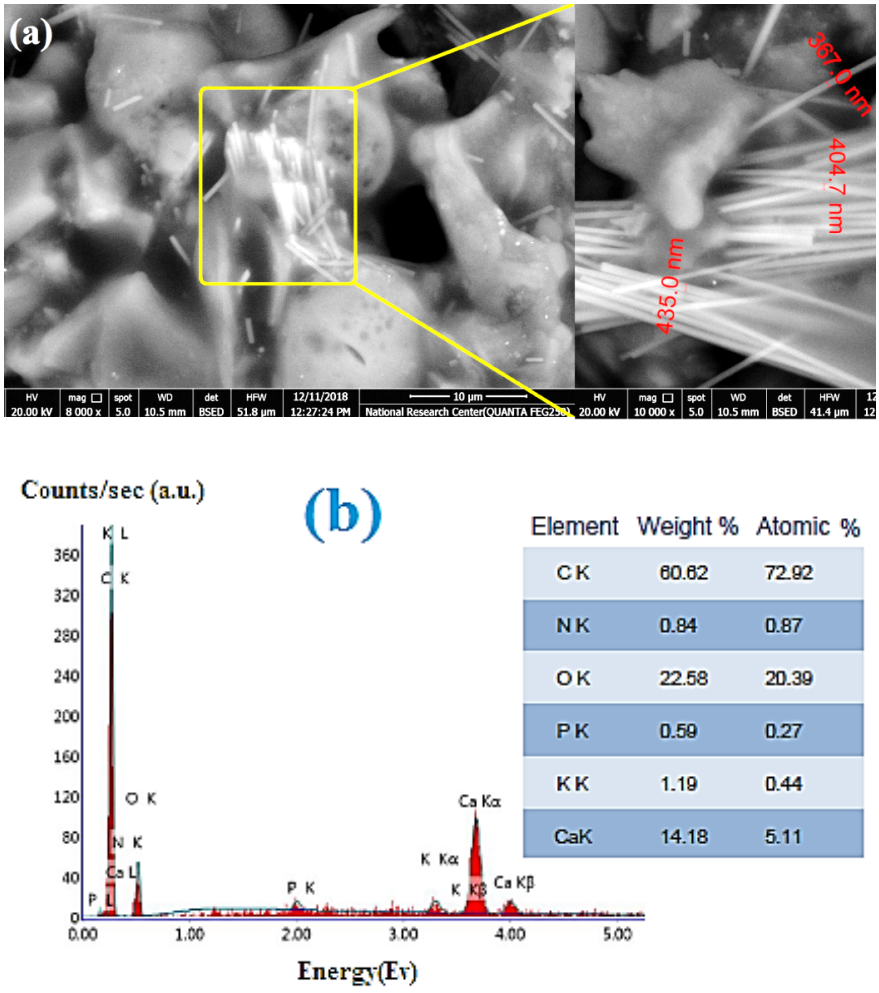

Figure 1. a) FESEM images for grapes seeds extract powder, b) EDAX analysis

EDAX analysis indicates the elemental analysis of the grape's seed powder. The powder is composed of 60% carbon from the cellulosic content along with nitrogen. Additionally, trace amounts of phosphorus, calcium, and potassium are depicted.

X-Ray Diffraction XRD

The crystalline structure of the grape seed powder was investigated via XRD diffractometry (Figure 2). The XRD pattern shows two diffraction peaks at 2 theta = 6.652˚, 20.73˚ indicating the crystalline nature of the tested powder. The two characteristic peaks are attributed to the cellulosic content within the grapes seeds powder.

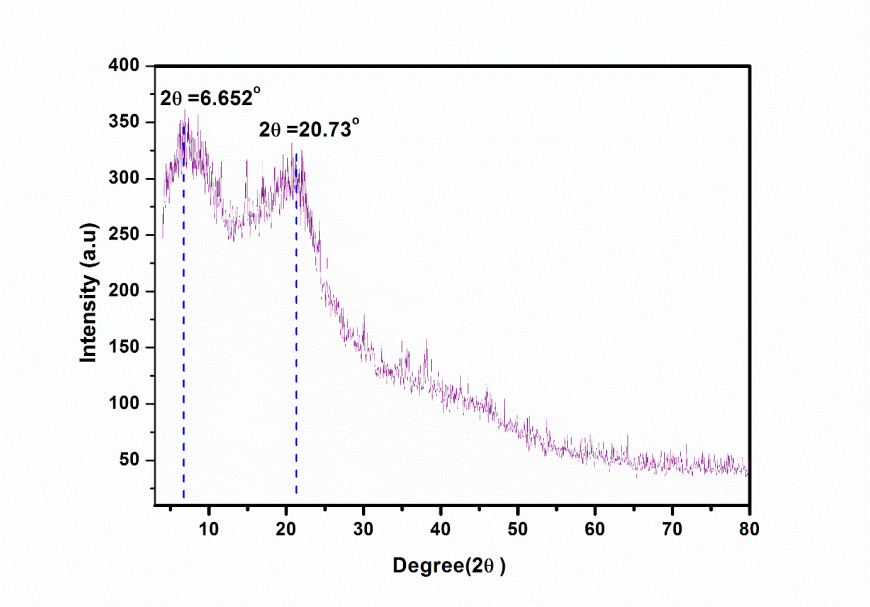

Figure 2. XRD pattern of the grapes seed extract powder

X-Ray Photon Spectroscopy (XPS)

XPS Survey narrow scan spectra of the ground grape seeds extract are represented in Figure 3. The main peaks of oxygen binding energies are located at 510 eV. Moreover, C 1s binding energies are depicted at 285 eV.

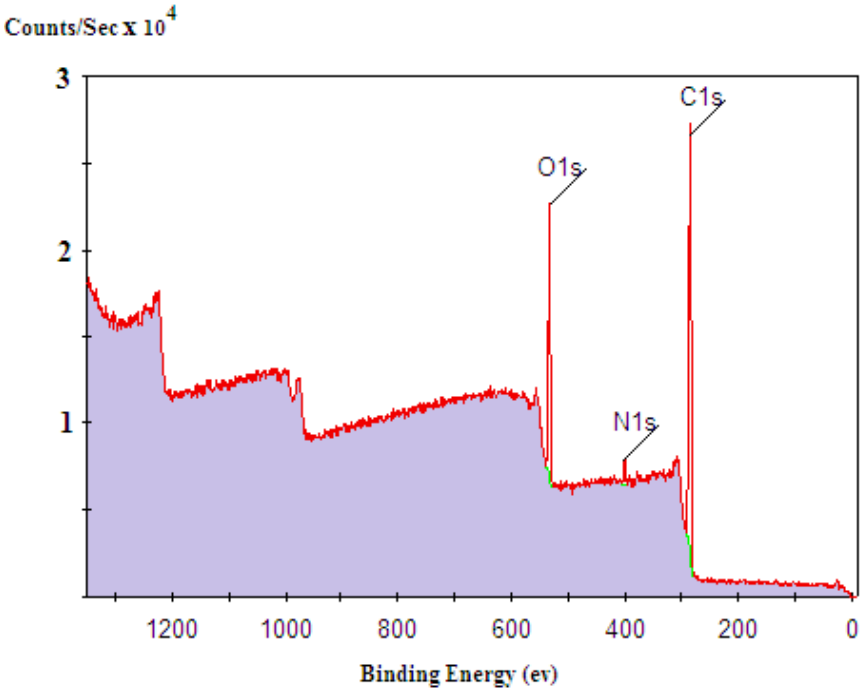

Figure 3. XPS of Grape Seeds Powder

Biological Implications

Antioxidant Activity

Grape seed extract's pharmacological importance as an antioxidant, anti-inflammatory, and anti-cancer activity is attributed to its high total phenolic and flavonoid content. Total phenolic concentration within grapes seed extract

was measured to be 90.5 mg gallic acid equivalents/g of extract. Moreover, total flavonoids exhibited a high value of 58 mg quercetin equivalents/g of extract. The recorded high concentrations exhibit promising antioxidant activity for grapes seed extracted by ultrasonic technique proving it is a reliable route for grapes seed extraction without affecting its antioxidant activity.

Free radical scavenging ability is used for the treatment of reperfusion tissue injuries even post-transplantation processes because of its anti-inflammatory ability and the reduction of apoptotic cell death [39, 40]. Grape seed extract contains powerful free radical scavengers (polyphenols) such as procyanidins and proanthocyanidins [41]. Grapes seed extraction inhibition percentage was measured by DPPH against ascorbic acid (Figure 4). Interestingly, grapes seed extract recorded a very high percentage of 91.29% at a concentration of 250 (ug/mL) competing with the most known free radical scavenger (ascorbic acid). Upon decreasing concentration; the inhibition percentage decreases. However, it still records promising inhibition ability.

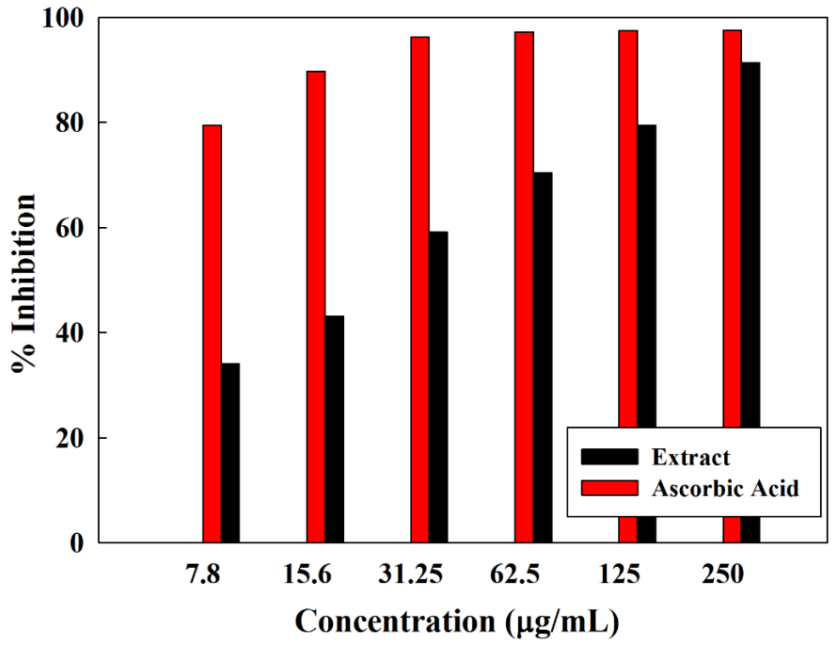

Figure 4. Grapes seeds extraction inhibition percentage against ascorbic acid

Bactericidal Activity

The agar diffusion technique was employed to investigate the prepared natural extract's bactericidal properties against tested bacterial strains. The achieved results revealed that the prepared extract evidenced substantially greater potentiality for the ability to hinder a wide range of GN species under investigation, which would include *E. coli* O157, *P. aeruginosa,* and *K. pneumoniae* at a level of 20 mg/ mL with the ZOI becoming 25 ±0.14, 26 ±0.28 and 28±0.23 mm, respectively, utilizing disc diffusion assay and ZOI becoming 27 ±0.14, 29 ±0.24 and 30±0.12. Using a disc diffusion experiment, the ZOI values of the extract against the GP species such as *S. aureus, B. subtilis,* and *L. monocytogenes* were concurrently verified to be 22 ±0.26, 20 ±0.16, and 21 ±0.22 mm, correspondingly (Table 1). The obtained results also exhibited that the studied extract was more powerful against GN bacteria than it was against GP bacteria.

Table 1. Measuring of ZOI diameters of the prepared natural extract against established dangerous bacterial strains

Tested dangerous bacterial species	ZOI diameter (mm)	
	Disc assay	Well assay
E. coli O157	25 ±0.14	27 ±0.14
P. aeruginosa	26 ±0.28	29 ±0.24
K. pneumoniae	28±0.23	30±0.12
S. aureus	22 ±0.26	25 ±0.21
B. subtilis	20 ±0.16	23 ±0.23
L. monocytogenes	21 ±0.22	24 ±0.16

The diameter of ZOI surrounding discs was discovered to be shorter than around wells, according to the findings. These findings are compatible with those of El Nahrawy *et al.,* [42, 43] who discovered that the ZOI width in the well diffusion assay is greater than that found in the Kirby -Bauer disk diffusion assay. Vancomycin, employed as a standard drug, has a shorter ZOI than the produced natural extract. This implies that perhaps the studied natural extract has stronger suppressive activity than the standard drug.

Estimation of MIC and IC_{50}

The MIC measurement was then applied to empirically validate the bactericidal activity of the various doses of the prepared natural extract. It is interesting to observe that, as depicted in figure 5, the prepared natural extract seemed to have a magnificent antibacterial influence against all tested microorganisms with varying MIC values of MICs relying on dosages (mg/mL) and retention time (min). Experimental findings of MIC values pointed out that the extract really had a strong antibacterial impact against *E.coli*, with 20 mg/mL of MIC after 20 min of exposure time, and 10 min for *P.aeruginosa* and *K.pneumoniae*. In other hand, the MIC values of *S.aureus* (MIC = 50 mg/mL after 20 min of exposure time). According to the findings, plant extract had lower MIC values for GN bacteria than GP bacteria (Table 2), (Figure 6). The discrepancy in inactivation properties might well be attributed to differences in the chemical components of the cells of bacteria and their potential to penetrate bacterial ' cellular membranes [44].

Table 2. The considered IC_{50}, Log IC_{50}, and R^2 of the prepared natural extract

The prepared natural extract	The prepared natural extract		
	IC_{50} (μM)	Log IC_{50} (μM)	R^2
E. coli O157	11.21	1.35	0964
P. aeruginosa	5.52	1.02	0.945
K. pneumoniae	8.24	1.21	0.936
S. aureus	12.65	1.40	0.978
B. subtilis	13.33	1.43	0.983
L.monocytogenes	16.69	1.50	0.965

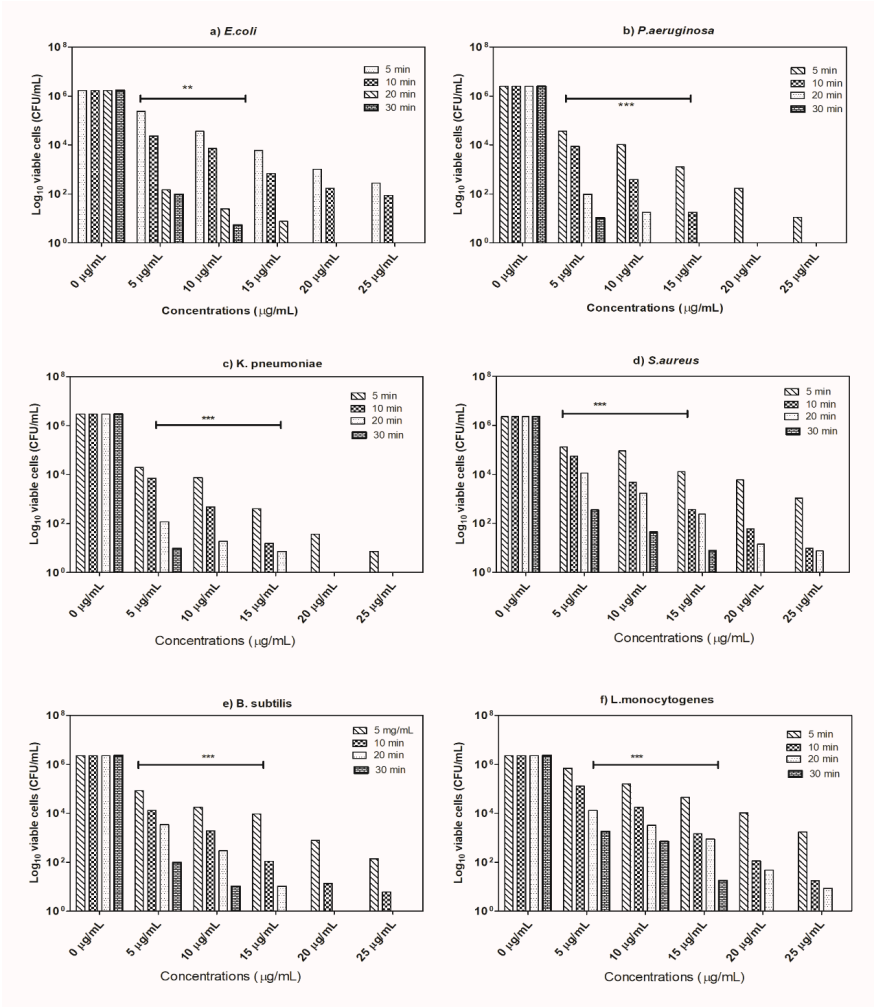

Figure 5. Estimated MIC values of the prepared natural extract towards examined bacterial species. The remaining viable cell populations are also shown at various time intervals of 5 min, 10, 15, and 30 min. Two-way analysis of variance (*ANOVA*) states ** indicates moderate correlation ($p \leq 0.01$), *** indicates high correlation ($p \leq 0.001$).

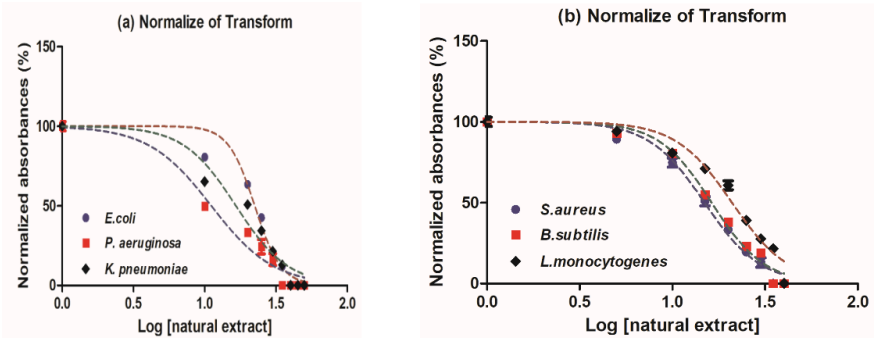

Figure 6. Normalized absorbance (%) of studied the prepared natural extract against a) Gram-negative and b) Gram-positive bacteria

The Kinetic Modeling Using the Pseudo-First-Order Kinetic Model

After becoming subject to the prepared extract, the examined bacterial species' deactivation probabilities were estimated using the pseudo-first-order reaction kinetics. Outcomes from kinetic simulations utilizing pseudo-first-order suggested that extract would swiftly prevent *P.aeruginosa* development, whereas *L.monocytogenes* organisms had the lowest suppression frequency. In addition, relying upon the type of microbial pathogens examined, the effective concentration of the natural extract was the one that could effectively suppress the growth of all bacterial

strains studied throughout a range of retention times. It was important to note that the *L.monocytogenes* species under investigation had massive damage over an extended period. The results obtained showed *that E.coli* > *P.aeruginosa* > *K.pneumoniae* > *S.aureus* > *B.subtilis* > *L.monocytogenes* tested the manufactured natural extract as a K_1 constant at a rapid rate of inactivation (Table 3).

Table 3. Kinetic values (K_1 (min^{-1})) of Pseudo-first-order calculation for inactivation of tested harmful bacterial strains by the prepared natural extract

Tested microbial pathogens	Prepared natural extract (25 µg/mL)	
	K_1	R^2
E. coli O157	0.4540	0.9634
P. aeruginosa	0.3649	0.9751
K. pneumoniae	0.3165	0.9952
S. aureus	0.2859	0.9847
B. subtilis	0.2348	0.9878
L. monocytogenes	0.1956	0.9893

The Physiological Altering of Bacterial Species

Following exposure to the effective dose of the prepared natural extract, the outcomes, as illustrated in figure 7, proved that the proliferation levels of all the tested bacterial species declined progressively and dramatically. The data attained determined that when comparing the bacterial growth curves of all analyzed bacteria, *P.aeruginosa* bacteria had a more significant and more rapid incline, whereas *L.monocytogenes* species had a lesser declining rate. Similarly, the amount of ATP is a powerful predictor of the productivity and vitality of the microbial species as well as the magnitude of their capability to proliferate, spread disease, and cause severe damage. Depending on the evidence in figure 8, *P.aeruginosa* bacteria had significantly lower levels of ATP compared to the other species subjected to the test, whereas *L.monocytogenes* bacteria displayed less of a drop.

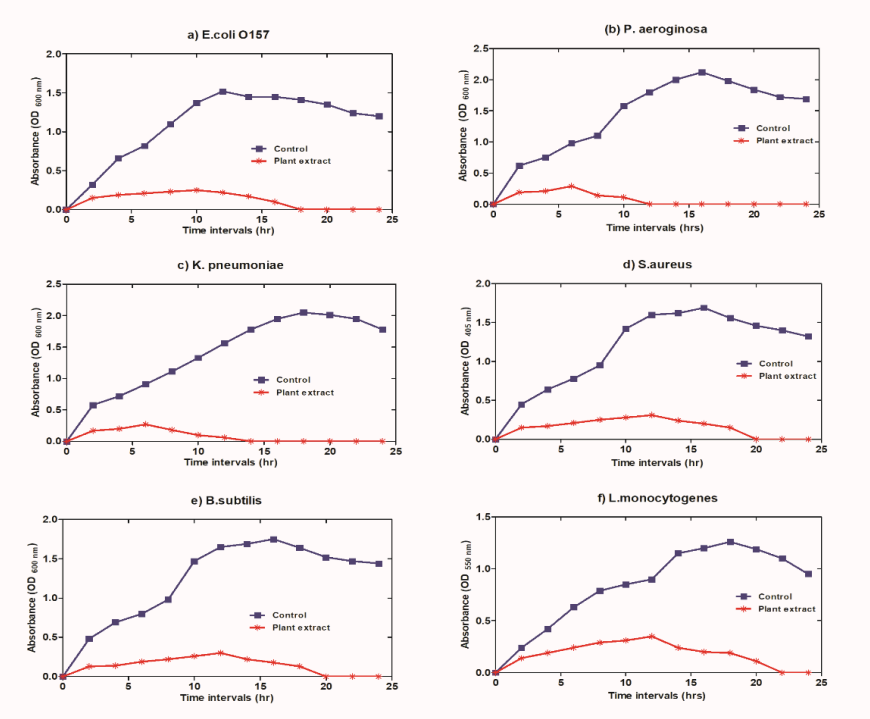

Figure 7. The growth curve of a) *E. coli O157*, b) *P.aeruginosa*, c) *K. pneumoniae* d) *S. aureus*, e) *B.subtilis*, f) *L.monocytogenes* before and after subjecting to the prepared natural extract

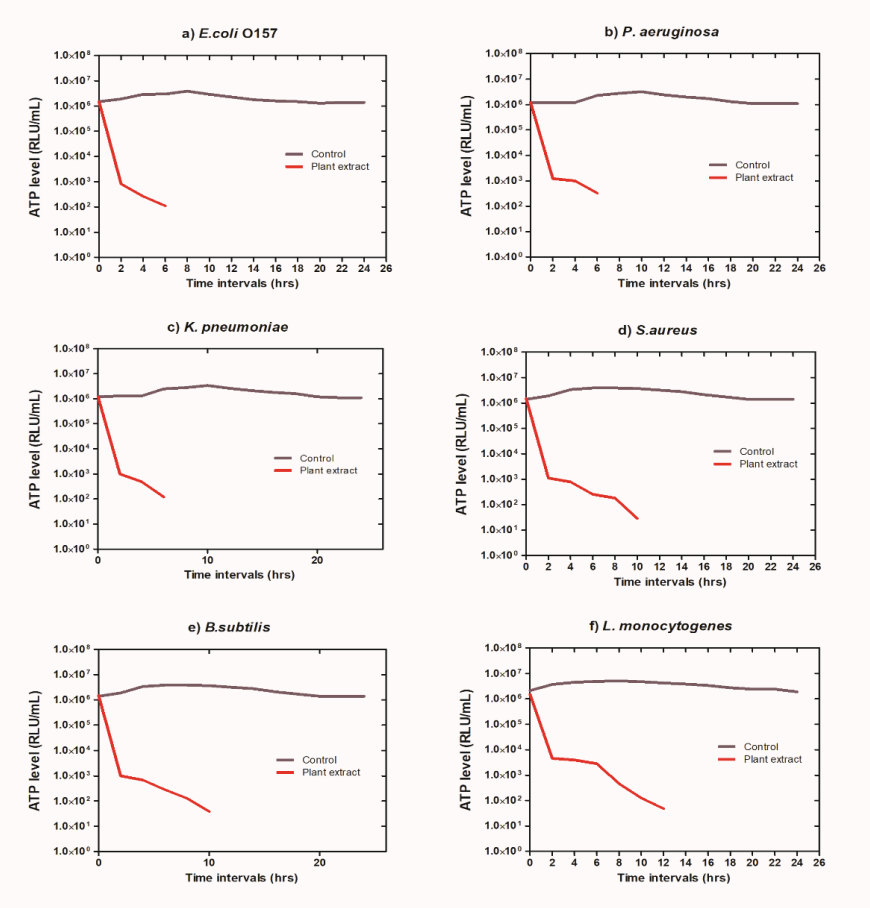

Figure 8. Amounts of ATP produced from a) *E. coli* O157, b) *P.aeruginosa*, c) *K. pneumoniae* d) *S. aureus*, e) *B.subtilis*, f) *L.monocytogenes* before and after subjecting to the prepared natural extract

Protein Release

As shown in Figure 9, the observations on protein permeability from damaged bacterial species revealed that the quantity of protein released massively increased following the potent dosage of the extract. As an indication of GN bacteria, protein leakage quantities increased for *P.aeruginosa,* and it was more substantial than for other species.

This evidence supports (Jiang *et al.* 2019) [45], who reported that the protein release rate and quantities from compromised E. coli cells were quicker and more significant than those unearthed in *S. aureus.* This is because disrupted *E.coli* cells have a small cell wall, highly permeable interlayer frameworks, and the structure of sluggish peptidoglycans. Consequently, it might be assumed that this type of natural extract might result in measurable cell substance ejection as well as critical morphological changes in the microbial cell wall [46]. GN bacteria with inadequate resilience to environmental stress include *P. aeruginosa* and *E. coli.* As a result of the absence of bacterial structures, they suffer loss or deformity. Antimicrobial drugs generate softly porous bacterial cells [47].

In contrast, the cell wall GN bacterial strains comprise 90% or more peptidoglycan, giving their walls more enduring physiological qualities. The prepared natural extract will become less effective against certain bacteria species as a result [48]. The incline of the curve of bacterial evolution and the amounts of proteins released as a result of cell lysis were significantly higher in Gram-negative bacteria than in GP bacteria, according to many pieces of evidence. This happens because the GP cell wall has a rigid and immovable structure that makes it more tolerant to bacteriostatic substances [49, 50].

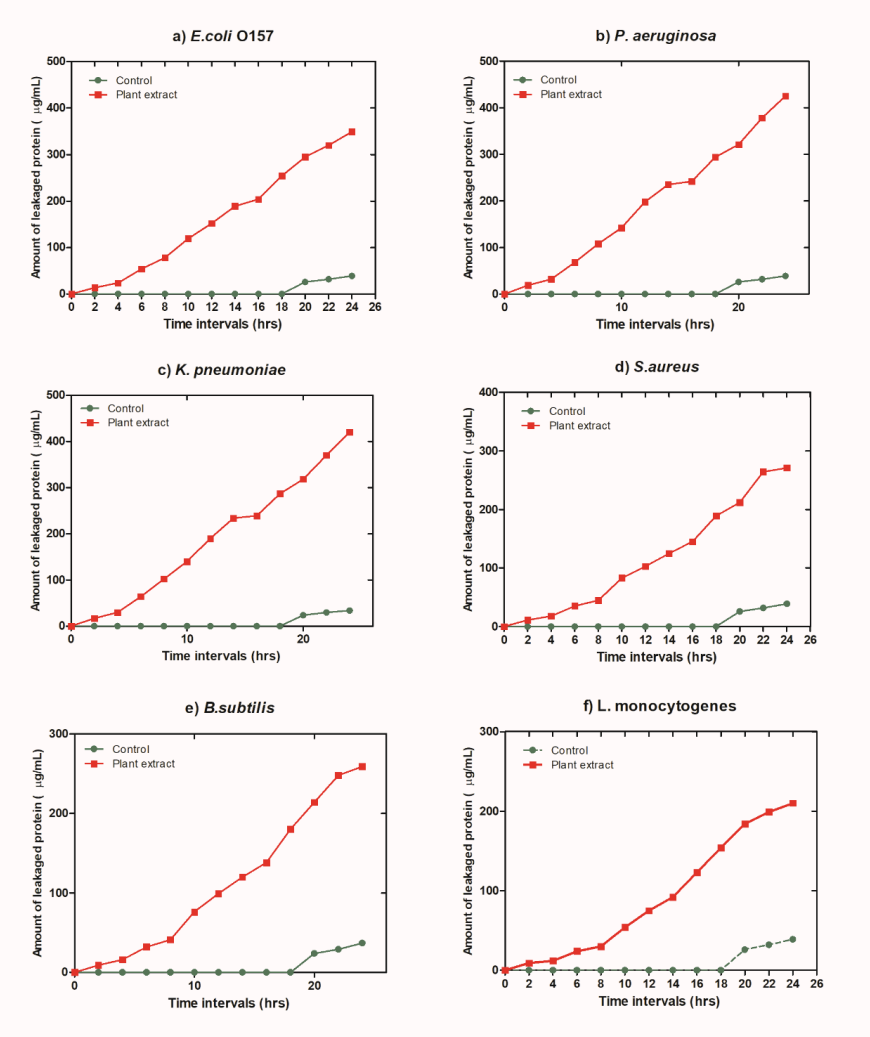

Figure 9. Quantities of the leakaged protein from a) *E. coli* O157, b) *P.aeruginosa,* c) *K. pneumoniae* d) *S. aureus,* e) *B.subtilis,* f) *L.monocytogenes* before and after subjecting to the prepared natural extract

Anti-Cancer Activity

Anticancer activity of the ultrasonic-assisted grapes seed extract was examined against normal Skin fibroblast (BJ1), Pancreatic cancer cell line (PACA2), Lung carcinoma cell line (A549), and Human Caucasian breast adenocarcinoma MCF7. The results proved the selective activity of the extract on a normal cell line by an inhibition ratio of 12.3%. An obvious reduction percentage of 78.2 % was recorded for PACA2 cells. Moreover, MCF7 was reduced by 65.3 %. The A549 had the lowest inhibition ratio of 25.2 at 100 ppm. The obtained results proved the cancer chemopreventive potential of the synthesized extract against tested cell lines. However, the variations in the inhibition percentage are due to the different anticancer mechanisms against cancer cell lines. The extract's anticancer activity mainly depends on its antioxidant activity. The promising anti-cancer activity of grapes seed extract is attributed to its high content of procyanidin dimers, especially procyanidin B2 as it is responsible for inhibition of the activity and expression of aromatase enzyme. Consequently, inhibits the conversion of androgens into estrogens in aromatase-transfected breast cancer cells and their xenografts [51, 52]. Additionally, Grapes seed extract proved to significantly reduce the metastatic nodules on the lung cancer cells surface [53]. Moreover, it exerts anti-proliferative and anti-angiogenic effects, thereby exerting growth inhibitory effect thus resulting in induction of apoptotic activity [54].

CONCLUSION

Egyptian grapes seed powder was characterized to investigate its structure as each country has its agricultural conditions. The obtained grape seeds were successfully extracted via an ultra-sonication probe at a power of 6 KJ for ten minutes only. The sonication technique proved its ability to preserve the grapes seed extract functional flavonoids as well as the other effective constituents. The obtained extract exhibits promising antioxidant activity as the measured total flavonoid content recorded a high value of 58 mg quercetin equivalents/g. Moreover, grape seed extract recorded a promising free radical scavenging percentage of 91.29 competing with ascorbic acid as most a free radical scavenger. Additionally, promising bactericidal activity against Gram-negative compared to Gram-positive bacteria due to the difference in their cell wall structure. Further, the anticancer activity results proved the selectivity of the extract on PACA2 cells with an inhibition percentage of 78.2 % followed by 65.3 % for MCF7 while the lowest inhibition ratio of 25.2 was recorded for A549.

STATEMENTS AND DECLARATIONS

Authors' Contributions

Walid El Hotaby is responsible for practical experiments and physicochemical characterization along with data interpretations; Bahaa Hemdan is responsible for bactericidal activity assessment and data interpretations; Wafa I. Abdel-Fattah is responsible for practical experiments and physicochemical characterization along with data interpretations; and Ghareib W. Ali responsible for practical experiments and physicochemical characterization along with data interpretations.

Competing Interests

The authors declare no competing interests.

Ethics Approval

The National Research Centre ethics committee granted official approval to carry out experiments involving human tissue.

Data Availability

The authors confirm that the data supporting the findings of this study are available within the article.

Funding

No funding was received to support this work.

ACKNOWLEDGMENTS

The financial support for the present study is appreciated by the authors through the running research project entitled “Metal cross-linked oxygenated multi-layer polymeric scaffold for Diabetic foot ulcer Wound Healing” application for a joint research grant under the India-Egypt agreement on science and technology cooperation.

AUTHORS’ INFORMATION

Walid El Hotaby—*Spectroscopy Dept., Physics Research Institute, National Research Centre, Egypt.*
Bahaa Hemdan—*Water Pollution Research Dept., Environmental Division, National Research Centre, Egypt.*
Wafa I. Abdel-Fattah—*Refractories, Ceramics, Building Materials, Dept. Biomaterials Group, Institute of advanced materials technology and mineral resources, National Research Centre, Egypt.*
Ghareib W. Ali—*Refractories, Ceramics, Building Materials, Dept. Biomaterials Group, Institute of advanced materials technology and mineral resources, National Research Centre, Egypt.*

REFERENCES

[1] A. Viveros, S. Chamorro, M. Pizarro, I. Arija, C. Centeno, A. Brenes, Effects of dietary polyphenol-rich grape pr oducts on intestinal microflora and gut morphology in broiler chicks, Poult Sci 90 (2011) 566–578. *https://doi.org/10.3382/PS.2010-00889*.

[2] P. Tataridis, E. Nerantzis, Integrated Enology Utilization of winery by-products into high added value product s, (n.d.). *https://www.academia.edu/8525686/Integrated_Enology_Utilization_of_winer* y_by_products_into_high_a dded_value_products (accessed January 3, 2022).

[3] A. Scalbert, G. Williamson, Dietary intake and bioavailability of polyphenols, J Nutr 130 (2000). *https://doi.org/10.1093/JN/130.8.2073S*.

[4] N. Sebastian, T.S. Ashwini, B. Mahendran, H.K. Sowmya, Evaluation and comparison of the efficiency of ultras onically activated intracanal irrigants grapeseed and pineapple extract in removing smear layer from the api cal third of the root canal: An in vitro SEM analysis, Endodontology 36 (2024) 251– 256. *https://doi.org/10.4103/ENDO.ENDO_129_23*.

[5] (20) (PDF) Can We Trust Trust? Diego Gambetta, (n.d.). *https://www.researchgate.net/publication/255682316_Can_We_Trust_Trust_Di* ego_Gambetta (accessed October 23, 2022).

[6] M. Monagas, C. Gómez-Cordovés, B. Bartolomé, Evolution of the phenolic content of red wines from Vitis vini fera L. during ageing in bottle, Food Chem 95 (2006) 405–412. *https://doi.org/10.1016/J.FOODCHEM.2005.01.004*.

[7] W.I. Abdel Fattah, Grape Seeds the Nontraditional Source for Achieving BioNanomaterials Addressing Antiba cterial, Anticancer and Antidiabetic Functions, Research & Development in Material Science 14 (2020). *https://doi.org/10.31031/RDMS.2020.14.000846*.

[8] S. Azizi, S.M. Nazari, L. MoradiHaghgou, Optimizing the Extraction of Antioxidant Components from Grape (V itis vinifera L.) Skin by Ultrasonic Pre-treatment, Journal of Food Science and Technology (Iran) 21 (2024) 118–137. *https://doi.org/10.22034/FSCT.21.146.118*.

[9] J.F. Hammerstone, S.A. Lazarus, H.H. Schmitz, Procyanidin Content and Variation in Some Commonly Consu med Foods, J Nutr 130 (2000) 2086S- 2092S. *https://doi.org/10.1093/JN/130.8.2086S*.

[10] M.D. Lucock, P.D. Roach, The antifolate activity of tea catechins., Undefined 65 (2005) 8573. *https://doi.org/10.1158/0008-5472.CAN-05-1414*.

[11] S. Spina, M.R. Farlow, F.W. Unverzagt, D.A. Kareken, J.R. Murrell, G. Fraser, F. Epperson, R.A. Crowther, M.G. Spi llantini, M. Goedert, B. Ghetti, The tauopathy associated with mutation +3 in intron 10 of Tau: characterizatio n of the MSTD family, Brain 131 (2008) 72–89. *https://doi.org/10.1093/BRAIN/AWM280*.

[12] M.J. Vallejo, L. Salazar, M. Grijalva, Oxidative stress modulation and ROSmediated toxicity in cancer: A review on in vitro models for plant-derived compounds, Oxid Med Cell Longev 2017 (2017). *https://doi.org/10.1155/2017/4586068*.

[13] A.M.L. Seca, D.C.G.A. Pinto, Plant Secondary Metabolites as Anticancer Agents: Successes in Clinical Trials and Therapeutic Application, Int J Mol Sci 19 (2018). *https://doi.org/10.3390/IJMS19010263*

[14] A. Gollucke, R. Peres, O. Jr, D. Ribeiro, Polyphenols: a nutraceutical approach against diseases, Recent Pat Foo d Nutr Agric 5 (2013) 214–219. *https://doi.org/10.2174/22127984056661311291532 39*.

[15] S.K. Katiyar, M. Athar, Grape seeds: ripe for cancer chemoprevention, Cancer Prev Res (Phila) 6 (2013) 617–62 1. *https://doi.org/10.1158/1940-6207.CAPR-* 13-0193.

[16] M. Jang, L. Asnin, S.H. Nile, Y.S. Keum, H.Y. Kim, S.W. Park, Ultrasoundassisted extraction of quercetin from on ion solid wastes, Int J Food Sci Technol 48 (2013) 246–252. *https://doi.org/10.1111/J.1365-2621.2012.03180.X*.

[17] M. Paini, A.A. Casazza, B. Aliakbarian, P. Perego, A. Binello, G. Cravotto, Influence of ethanol/water ratio in ult rasound and high-pressure/hightemperature phenolic compound extraction from agri-food waste, Int J Food Sci Technol 51 (2016) 349–358. *https://doi.org/10.1111/IJFS.12956*.

[18] B. Kumari, B.K. Tiwari, M.B. Hossain, D.K. Rai, N.P. Brunton, Ultrasoundassisted extraction of polyphenols fro m potato peels: profiling and kinetic modelling, Int J Food Sci Technol 52 (2017) 1432–1439. *https://doi.org/10.1111/IJFS.13404*.

[19] S. Chaji, G. Capaldi, L. Gallina, G. Grillo, L. Boffa, G. Cravotto, Semiindustrial ultrasound-assisted extraction of grape-seed proteins, J Sci Food Agric 104 (2024) 5689–5697. *https://doi.org/10.1002/JSFA.13395*.

[20] A.M. Bakr, B. Anis, W.M. El Hotaby, Sounchemical synthesis of Graphene/nano hydroxyapatite composites for potential biomedical application, Egypt J Chem 65 (2022) 669–678. *https://doi.org/10.21608/EJCHEM.2021.91241.4339*.

[21] L. Sun, H. Wang, J. Du, T. Wang, D. Yu, Ultrasonic-assisted extraction of grape seed procyanidins, preparation of liposomes, and evaluation of their antioxidant capacity, Ultrason Sonochem 105 (2024) 106856. *https://doi.org/10.1016/J.ULTSONCH.2024.106856*.

[22] F.J. Barba, Z. Zhu, M. Koubaa, A.S. Sant'Ana, V. Orlien, Green alternative methods for the extraction of antioxidant bioactive compounds from winery wastes and by-products: A review, Trends Food Sci Technol 49 (2016) 96–109. *https://doi.org/10.1016/J.TIFS.2016.01.006*.

[23] K.E.L. Mazza, M.C.P.A. Santiago, L.S.M. do Nascimento, R.L.O. Godoy, E.F. Souza, A.I.S. Brígida, R.G. Borguini, R. V. Tonon, Syrah grape skin valorisation using ultrasound-assisted extraction: Phenolic compounds recovery, antioxidant capacity and phenolic profile, Int J Food Sci Technol 54 (2019) 641–650. *https://doi.org/10.1111/IJFS.13883*.

[24] W. El Hotaby, A.M. Bakr, H.H.A. Sherif, A.A. Soliman, B. Hemdan, Exploring the antimicrobial and anticancer activities of zinc doped nanohydroxyapatite prepared via ultrasonic-assisted method for bone tissue engineering, J Mater Res 39 (2024) 1911–1925. *https://doi.org/10.1557/S43578-024-01350-4/TABLES/2*.

[25] E. Pastrana-Bonilla, C.C. Akoh, S. Sellappan, G. Krewer, Phenolic Content and Antioxidant Capacity of Muscadine Grapes, J Agric Food Chem 51 (2003) 5497–5503. *https://doi.org/10.1021/JF030113C*.

[26] S. Haida, A. Kribii, Chemical composition, phenolic content and antioxidant capacity of Haloxylon scoparium extracts, South African Journal of Botany 131 (2020) 151–160. *https://doi.org/10.1016/J.SAJB.2020.01.037*.

[27] A. Pękal, K. Pyrzynska, Evaluation of Aluminium Complexation Reaction for Flavonoid Content Assay, Food Anal Methods 7 (2014) 1776–1782. *https://doi.org/10.1007/S12161-014-9814-X/TABLES/2*.

[28] S.A. Baba, S.A. Malik, Determination of total phenolic and flavonoid content, antimicrobial and antioxidant activity of a root extract of Arisaema jacquemontii Blume, *Https://Doi.Org/10.1016/j.Jtusci.2014.11.001* 9 (2018) 449–454. *https://doi.org/10.1016/J.JTUSCI.2014.11.001*.

[29] G.W. Ali, W. El-Hotaby, B. Hemdan, W.I. Abdel-Fattah, Thermosensitive chitosan/phosphate hydrogel-composites fortified with Ag versus Ag@Pd for biomedical applications, Life Sci 194 (2018) 185–195. *https://doi.org/10.1016/J.LFS.2017.12.021*.

[30] A.M. El Nahrawy, B.A. Hemdan, A.B. Abou Hammad, A.L.K. Abia, A.M. Bakr, Microstructure and Antimicrobial Properties of Bioactive Cobalt CoDoped Copper Aluminosilicate Nanocrystallines, Silicon 2019 12:10 12 (2019) 2317–2327. *https://doi.org/10.1007/S12633-019-00326-Y*.

[31] M. Lavorgna, R. Iacovino, C. Russo, C. Di Donato, C. Piscitelli, M. Isidori, A New Approach for Improving the Antibacterial and Tumor Cytotoxic Activities of Pipemidic Acid by Including It in Trimethyl-β-cyclodextrin, Int J Mol Sci 20 (2019). *https://doi.org/10.3390/IJMS20020416*.

[32] A.M. El Nahrawy, A. Elzwawy, M.M. Alam, B.A. Hemdan, A.M. Asiri, M.R. Karim, A.B.A. Hammad, M.M. Rahman, Synthesis, structural analysis, electrochemical and antimicrobial activities of copper magnesium zirconosilicate (Cu20Mg10Si40Zr(30-x)O:(x = 0,5,7,10) Ni2+) nanocrystals, Microchemical Journal 163 (2021) 105881. *https://doi.org/10.1016/J.MICROC.2020.105881*.

[33] D.F. Sargent, H.J. Moeschler, Determination of pseudo-first-order reaction kinetics by batch microcalorimetry, Anal Chem 52 (1980) 365–367. *https://doi.org/10.1021/AC50052A042/ASSET/AC50052A042.FP.PNG_V03*.

[34] A.M. El Nahrawy, A.B.A. Hammad, A.M. Bakr, B.A. Hemdan, A.R. Wassel, Decontamination of ubiquitous harmful microbial lineages in water using an innovative Zn2Ti0.8Fe0.2O4 nanostructure: dielectric and terahertz properties, Heliyon 5 (2019) e02501. *https://doi.org/10.1016/J.HELIYON.2019.E02501*.

[35] A.M. El Nahrawy, B.A. Hemdan, A.B. Abou Hammad, A.M. Othman, A.M. Abouelnaga, A.M. Mansour, Modern Template Design and Biological Evaluation of Cephradine-loaded Magnesium Calcium Silicate Nanocomposites as an Inhibitor for Nosocomial Bacteria in Biomedical Applications, Silicon 2020 13:9 13 (2020) 2979–2991. *https://doi.org/10.1007/S12633-020-00642-8*.

[36] M. He, T. Wu, S. Pan, X. Xu, Antimicrobial mechanism of flavonoids against Escherichia coli ATCC 25922 by model membrane study, Appl Surf Sci 305 (2014) 515–521. *https://doi.org/10.1016/J.APSUSC.2014.03.125*.

[37] B.A. Hemdan, A.M. El Nahrawy, A.F.M. Mansour, A.B.A. Hammad, Green sol–gel synthesis of novel nanoporous copper aluminosilicate for the eradication of pathogenic microbes in drinking water and wastewater treatment, Environmental Science and Pollution Research 26 (2019) 9508–9523. *https://doi.org/10.1007/S11356-019-04431-8/FIGURES/10*.

[38] B.A. Hemdan, M.A. El-Liethy, A.M. Shaban, G.E.S. El-Taweel, Quantification of the metabolic activities of natur al biofilm of different microenvironments, Journal of Environmental Science and Technology 10 (2017) 131–1 38. *https://doi.org/10.3923/JEST.2017.131.138*.

[39] S.Q. Li, Q. Howard Zhang, Advances in the development of functional foods from buckwheat, Crit Rev Food Sc i Nutr 41 (2001) 451–464. *https://doi.org/10.1080/20014091091887*.

[40] M. Sato, S. Fujisaki, K. Sato, Y. Nishimura, A. Nakano, Yeast Saccharomyces cerevisiae has two cis-prenyltransf erases with different properties and localizations. Implication for their distinct physiological roles in dolichol synthesis, Genes to Cells 6 (2001) 495–506. *https://doi.org/10.1046/j.1365-* 2443.2001.00438.x.

[41] D. Bagchi, M. Bagchi, S.J. Stohs, D.K. Das, S.D. Ray, C.A. Kuszynski, S.S. Joshi, H.G. Pruess, Free radicals and gra pe seed proanthocyanidin extract: Importance in human health and disease prevention, Toxicology 148 (200 0) 187–197. *https://doi.org/10.1016/S0300-483X(00)00210-9*.

[42] A.M. El Nahrawy, B.A. Hemdan, A.M. Mansour, A. Elzwawy, A.B. Abou Hammad, Integrated use of nickel cobal t aluminoferrite/Ni2+ nano-crystallites supported with SiO2 for optomagnetic and biomedical applications, Materials Science and Engineering: B 274 (2021) 115491. *https://doi.org/10.1016/J.MSEB.2021.115491*.

[43] M.M.H. El-Sayed, A.A. Mostafa, A.M. Gaafar, W. El Hotaby, E.M.A. Hamzawy, M.S. El-Okaily, A.M. Gamal-Eldeen, In vitro kinetic investigations on the bioactivity and cytocompatibility of bioactive glasses prepared via meltin g and sol-gel techniques for bone regeneration applications, Biomedical Materials (Bristol) 12 (2017). *https:// doi.org/10.1088/1748-605X/aa5a30*.

[44] S.T. Gaballah, H.A. El-Nazer, R.A. Abdel-Monem, M.A. El-Liethy, B.A. Hemdan, S.T. Rabie, Synthesis of novel chit osan-PVC conjugates encompassing Ag nanoparticles as antibacterial polymers for biomedical applications, Int J Biol Macromol 121 (2019) 707–717. *https://doi.org/10.1016/J.IJBIOMAC.2018.10.085*.

[45] Y. Jiang, J. Chen, K. Yen, J. Xu, Ectopically Expressed IL-34 Can Efficiently Induce Macrophage Migration to the Liver in Zebrafish, Zebrafish 16 (2019) 165–170. *https://doi.org/10.1089/ZEB.2018.1685*.

[46] Y. Xie, Y. He, P.L. Irwin, T. Jin, X. Shi, Antibacterial activity and mechanism of action of zinc oxide nanoparticles against Campylobacter jejuni, Appl Environ Microbiol 77 (2011) 2325–2331. *https://doi.org/10.1128/AEM.02149* - 10.

[47] W. Vollmer, D. Blanot, M.A. De Pedro, Peptidoglycan structure and architecture, FEMS Microbiol Rev 32 (2008) 149–167. *https://doi.org/10.1111/J.1574-6976.2007.00094.X*.

[48] A.M. El Nahrawy, A.M. Bakr, B.A. Hemdan, A.B. Abou Hammad, Identification of Fe3+ co-doped zinc titanate mesostructures using dielectric and antimicrobial activities, International Journal of Environmental Science a nd Technology 17 (2020) 4481–4494. *https://doi.org/10.1007/S13762-020-* 02786-X/FIGURES/8.

[49] A.M.E. Nahrawy, A.M. Bakr, A.B.A. Hammad, B.A. Hemdan, High performance of talented copper/magneso-zi nc titanate nanostructures as biocidal agents for inactivation of pathogens during wastewater disinfection, A pplied Nanoscience (Switzerland) 10 (2020) 3585–3601. *https://doi.org/10.1007/S13204-020-01454-3/FIGURES/1 0*.

[50] A.B. Abou Hammad, B.A. Hemdan, A.M. El Nahrawy, Facile synthesis and potential application of Ni0.6Zn0.4F e2O4 and Ni0.6Zn0.2Ce0.2Fe2O4 magnetic nanocubes as a new strategy in sewage treatment, J Environ Man age 270 (2020) 110816. *https://doi.org/10.1016/J.JENVMAN.2020.110816*.

[51] A. Leone, C. Longo, C. Gerardi, J.E. Trosko, Pro-Apoptotic Effect of Grape Seed Extract on MCF-7 Involves Tran sient Increase of Gap Junction Intercellular Communication and Cx43 Up-Regulation: A Mechanism of Chem oprevention, Int J Mol Sci 20 (2019). *https://doi.org/10.3390/IJMS20133244*.

[52] H.M. Habib, E.M. El-Fakharany, E. Kheadr, W.H. Ibrahim, Grape seed proanthocyanidin extract inhibits DNA an d protein damage and labile iron, enzyme, and cancer cell activities, Scientific Reports 2022 12:1 12 (2022) 1– 14. *https://doi.org/10.1038/s41598-022-16608-2*.

[53] B. Xue, Q.Y. Lu, L. Massie, C. Qualls, J.T. Mao, Grape seed procyanidin extract against lung cancer: the role of microrna-106b, bioavailability, and bioactivity, Oncotarget 9 (2018) 15579–15590. *https://doi.org/10.18632/ON COTARGET.24528*.

[54] E.M. Kim, C.H. Jung, J. Kim, S.G. Hwang, J.K. Park, H.D. Um, The p53/p21 Complex Regulates Cancer Cell Invasi on and Apoptosis by Targeting Bcl-2 Family Proteins, Cancer Res 77 (2017) 3092–3100. *https://doi.org/10.115 8/0008-5472.CAN-16-2098*.